J. Biophotonics **7**, No. 9, 683–689 (2014) / **DOI** 10.1002/jbio.201300006

Journal of BIOPHOTONICS

FULL ARTICLE

Towards *in vivo* intradermal surface enhanced Raman scattering (SERS) measurements: silver coated microneedle based SERS probe

*Clement Yuen and Quan Liu**

Division of Bioengineering, School of Chemical and Biomedical Engineering, Nanyang Technological University, 70 Nanyang Drive, Singapore 637457, Singapore

Received 7 January 2013, revised 26 March 2013, accepted 21 April 2013
Published online 13 May 2013

Key words: Raman, surface enhanced Raman scattering (SERS), partial least squares (PLS), intradermal glucose measurement

We propose a microneedle coated with silver (Ag) to detect analytes at low concentrations positioned at a depth of more than 700 μm below the surface of a skin phantom with absorbers and scatterers for mimicking the intradermal surface-enhanced Raman scattering (SERS) measurements. The Ag layer in the Ag-coated microneedle-based probe is found to be the key to the effective detection of analytes buried inside the aforesaid phantom. Glucose concentrations ranging from 5 to 150 mM inside phantoms can be estimated with a root mean square error (RMSE) of 3.3 mM. This work shows the potential of using microneedles for simple *in vivo* intradermal SERS measurements of analytes with clinical relevance.

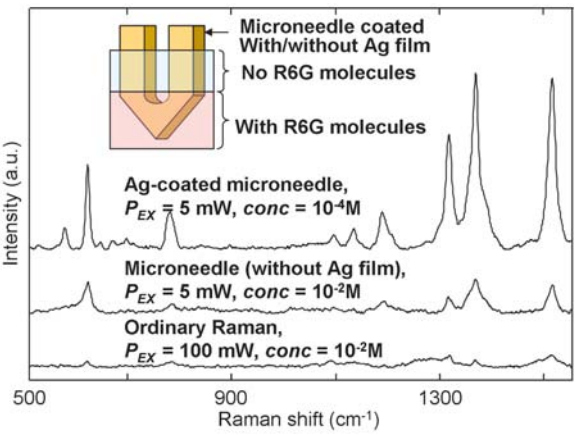

SERS spectra of R6G molecules positioned inside the bottom layer of an agar phantom at a depth of 760 μm below the surface (inset) measured by using Ag-coated microneedle (*conc*: 10^{-4} M; P_{EX}: 5 mW), microneedle (*conc*: 10^{-2} M; P_{EX}: 5 mW), and ordinary Raman (*conc*: 10^{-2} M; P_{EX}: 100 mW). P_{EX} means the excitation power and *conc* means concentration of R6G in the bottom layer.

* Corresponding author: e-mail: quanliu@ntu.edu.sg, Phone: +65 6316 8748, Fax: +65 6791 1761

1. Introduction

Characterizations of human intradermal components, e.g. dendritic cells and capillary blood, is important in the areas of immunology and diagnosis [1]. These components are buried at 700 μm under the human skin or deeper [2]. Fluorescence spectroscopy, magnetic resonance imaging, ultrasound and other techniques have been developed to probe intradermal layers [3, 4]. Among these methods, Raman spectroscopy promises to offer fingerprints related to structures, conformations, and processes in biomolecules below the skin [3]. Although Raman measurements can be achieved from a depth of about 200 μm under the skin [3], the measurements of dermal components deeper than 700 μm is difficult. Moreover, the detection sensitivity is limited by the small Raman scattering cross section (10^{-29}–10^{-32} cm^2) of endogenous biomolecules [5]. In contrast, surface-enhanced Raman scattering (SERS) technique can amplify Raman signals up to 10^{14} folds using metallic surfaces [e.g., silver (Ag) and gold] [6]. The SERS strategy has also demonstrated *in vivo* Raman measurements with penetration deeper than 700 μm, but the subcutaneous injection of metal nanoparticles can be toxic [7]. Though the use of SERS-active acupuncture needles can eliminate the need of nanoparticle injection [8], these needles are still required to be pulled out from the subject for SERS measurements and skillful needle administration is needed [8, 9]. Recently, microneedles have been used for intradermal drug delivery with the advantages in minimum pain and easy administration [10], which implies the potential of using microneedles for intradermal measurements. In this study, we propose an Ag-coated microneedle-based SERS probe to detect Rhodamine 6G and glucose test molecules buried deeper than 700 μm inside phantoms that are comprised of elastic scatterers and absorbers to mimic the human skin. To our best knowledge, the use of microneedles for *in situ* SERS measurements in skin phantoms has not been reported in the literature.

2. Methods and materials

2.1 Chemicals and reagents

Silver nitrate ($AgNO_3$) ($AgNO_3$, catalog no. 1.01512.0025) and sodium hydroxide pellets (NaOH, catalog no. 1.06498.1000) were purchased from Merck, Darmstadt, Germany. D-glucose anhydrous (catalog no. A16828) and 28% ammonium hydroxide (NH_4OH, catalog no. L13168) were ordered from Alfa Aesar, Massachusetts, USA. Agarose powder (catalog no. PC0701) was purchased from Vivantis, Selangor, Malaysia. Nigrosin, rhodamine 6G (R6G, catalog no. R4127) and 20% intralipid (catalog no. I141) were obtained from Sigma Aldrich, Missouri, USA. All chemicals used were of the analytical grade.

2.2 Preparation of Ag coated microneedle

We coated 750 nm thick Ag films onto microneedles in microneedle patches (AdminPatch® 1200 [10], AdminMed, California, USA) by using the Tollen's method. The Tollen's method was selected to synthesize the Ag films because effective SERS has been demonstrated in other Ag-film substrates [11] at 785 nm excitation using this method. The microneedle patch was placed in a solution mixed with 1.5 ml $AgNO_3$ at a concentration of 0.3 M and 0.75 ml NaOH at a concentration of 2.5 M. Precipitates formed in this mixture were redissolved by dropwise addition of 0.2 ml of concentrated NH_4OH. Glucose in a volume of 4.5 ml at a concentration of 0.1 M was subsequently introduced to reduce Ag ions to form the Ag film. After 15 minutes, the patch was taken out, rinsed with deionized water and dried up prior to testing.

2.3 Construction of phantom layers

To fabricate a 760 μm thick phantom layer, agarose powder was dissolved in deionized water after boiling in microwave oven (R369T(S), Sharp, Osaka, Japan). Nigrosin was added as an absorber at a concentration of 6 μM to yield an absorption coefficient of 0.5 cm^{-1} at 785 nm. This result was acquired by an ultraviolet-visible spectrophotometer (UV2450, Shimadzu, Kyoto, Japan). Intralipid-20% in a volume of 1.967 ml was added as elastic scatterers to an agarose phantom mixture with a total volume of 50 ml. A reduced scattering coefficient of 13 cm^{-1} was determined by a tissue oximeter (OxiplexTS, ISS, Champaign, Illinois, USA). The absorbers and scatterers were added into the agarose solution at about 60 °C to yield a 1% agarose phantom with a total volume of 50 ml to mimic the reported optical absorption and scattering properties [12] of human skin. The mixture was pipetted in between two glass slides with a 760 μm gap created by stacking four cover slips [Figure 1(a) and (b)]. The same recipe was also used to fabricate the bottom layer, and the agarose mixture was mixed with R6G (10^{-4}–10^{-6} M) or glucose (0–150 mM) at a range of concentrations at about 60 °C prior to setting in a Petri dish.

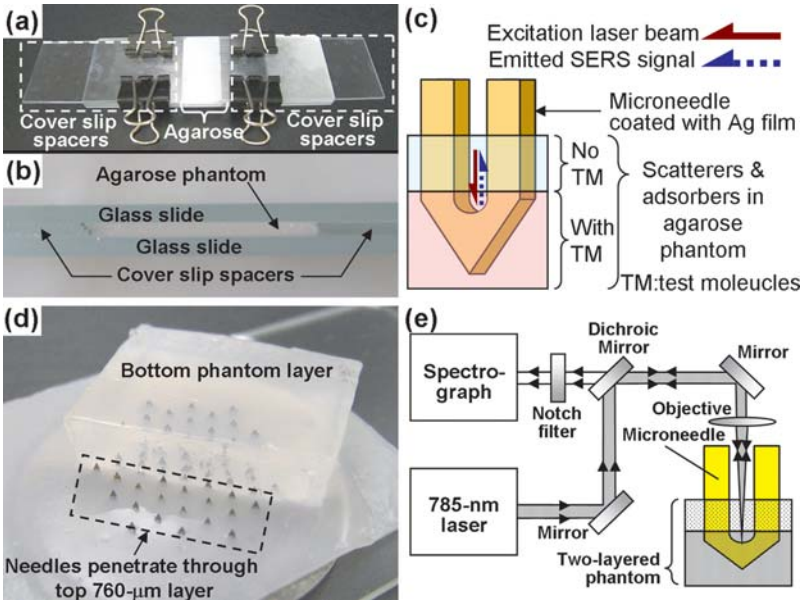

Figure 1 (**a**) Image and (**b**) side view of the setup for the fabrication of 760 μm thick top phantom layers. (**c**) Schematic of the Ag film coated microneedle probed into a two-layered phantom. (**d**) Microneedles penetrating through the top layer into the second layer. Note the phantom was placed upside down to facilitate the visualization of penetration. (**e**) Schematic of the Raman system for SERS measurements.

2.4 Raman instrumentation

In SERS measurements, the Ag film coated microneedle patch was pressed into the 760 μm thick top phantom layer stacked on top of the bottom phantom layer with test molecules [Figure 1(c)]. The microneedles penetrated through the top layer and pierced into the bottom layer. The penetration was clearly evident in Figure 1(d) in which R6G, intralipid and nigrosin were not introduced into the bottom layer. All samples were excited [Figure 1(e)] by a 785 nm laser (Renishaw, Gloucestershire, UK) with a power of 5 mW focused via a microscope objective (20×, NA = 0.4, Leica, Solms, Germany) at an optimal depth of 675 μm (as shown later in the results of Raman signal optimization by variation of focusing depth) in between the two arms of the microneedle below the surface of the top layer. Emitted SERS signal propagated in the opposite direction along the same optical path back to a Czerny-Turner type spectrograph ($f = 250$ mm). A holographic grating (1800 gr/mm) dispersed the signal into a Rem Cam CCD detector (inVia, Renishaw, Gloucestershire, UK) for analysis. The spectral resolution was 2 cm^{-1} and integration time was 10 s. These raw data underwent the baseline correction, followed by averaging over a five-point window to reduce noise and removal [13] of fluorescence background, which yielded the final spectra shown in the Results section.

2.5 Estimation of glucose concentrations

We utilized the partial least square (PLS) regression and a leave-one-out (LOO) technique [5, 14] to process all data points to assess the efficacy of the Ag-coated microneedle-based SERS probe in glucose concentration estimation. A public domain Matlab code [15] was modified to implement PLS–LOO analysis. Note that a total of 50 data points with the glucose concentrations ranging from 0 to 150 mM were examined in this study. In the PLS–LOO validation, one data point was left out to validate against the rest of the data points (49 data points). The glucose concentration for that one data point, C_{est}, was estimated from the Raman intensity using the reference regression line formed by the remaining 49 data points, which was then compared to the reference glucose concentrations, C_{ref}, for validation. This procedure was repeated by leaving out a different data point until the glucose concentrations corresponding to all data points have been estimated once. The root-mean-squared error of estimation (RMSE) [5],

$$\mathrm{RMSE} = \sqrt{\frac{1}{50}\sum_{i=1}^{50}(C_{\mathrm{est},\,i} - C_{\mathrm{ref},\,i})^2} \qquad (1)$$

was calculated to determine the accuracy of estimated glucose concentrations using this SERS technique, in which i is the index number of the data point.

2.6 Field emission scanning electronic microscope (FESEM) analysis

The Ag-coated microneedle was coated with a thin layer of platinum by using a fine coater (JOEL JFC-1600, JOEL, Japan), followed by the FESEM (JOEL JSM-6700F, JOEL, Japan) imaging with an accelerating voltage of 5 kV.

2.7 Discrete-dipole approximation modelling

We employed the discrete-dipole approximation (DDA) model [16] to calculate the extinction efficiency for the Ag morphologies on the microneedle. The surface morphologies (1.875 μm × 1.875 μm × 0.8 μm) acquired from FESEM image was discretized into cube-shaped dipoles with a side length of 25 nm to solve the Maxwell's equations of electromagnetic waves in the investigated volume in order to compute the extinction efficiencies (Q_{ext}) by using the Amsterdam DDA [16] code. Unpolarized plane wave was excited in a direction parallel to the surface normal of the substrate, into a volume assumed to be comprised of only Ag and air with electric constants obtained from a Ref. [17].

3. Results and discussion

Figure 2 compares the Raman spectra of R6G buried in the bottom phantom layer at 760 μm below the surface at concentrations ranging from 10^{-2} M to 10^{-6} M measured by the microneedle-based SERS probe in the cases of (a) with and (b) without Ag film coating. The ordinary Raman spectra were also shown in (c) for comparison. These spectra were averaged from five different locations with a signal standard deviation of less than 5%. Prominent Raman peaks located at about 615, 775, 1185, 1310, 1365, and 1508 cm^{-1}, which can be attributed to the C–C–C ring in-plane bending, CH out-of-plane bending, C–O–C stretching, C–C/C–N stretching and aromatic C–C stretching, respectively [13, 18], are observed in the R6G Raman spectra measured using the microneedle based SERS probe [Figure 2(a) and (b)]. In contrast, the ordinary Raman spectra of R6G at higher concentrations show only weak Raman peaks even at a higher excitation power of 100 mW. These measurement results obtained are acquired from the optimal depth below the surface of the two-layer phantom as given by the dependence of SERS intensity as a function of laser focusing depth below the surface of the top phantom layer [Figure 2(d)]. Note that the depth below the surface has been calibrated for the refractive index mismatch between the agarose phantom (with a refractive index of 1.35 [19]) and air. For depth from 270 to 675 μm, the intensity is increasing attributing to the fact that the excitation light is moving into the R6G layer. Contrarily, the intensity decreases as the focusing laser spot focused from 675 to 1620 μm, since the returning path for the emission becomes longer.

Base on these results, the analytical enhancement factor (AEF) of the Raman measurement in case of the microneedle (with or without Ag coating) with respect to the ordinary Raman measurement without the microneedle can be calculated using the following Ref. [13],

$$\mathrm{AEF} = \frac{I_{1508,\,\mathrm{Needle}}}{I_{1508,\,\mathrm{No\,Needle}}} \times \frac{P_{\mathrm{No\,Needle}}}{P_{\mathrm{Needle}}} \times \frac{C_{\mathrm{No\,Needle}}}{C_{\mathrm{Needle}}} \qquad (2)$$

where ($I_{1508,\ \mathrm{Needle}}/I_{1508,\ \mathrm{NoNeedle}}$), ($P_{\mathrm{Needle}}/P_{\mathrm{NoNeedle}}$), and ($C_{\mathrm{Needle}}/C_{\mathrm{NoNeedle}}$) are the ratios of the Raman intensities at a Raman shift of 1508 cm^{-1}, excitation powers, and R6G concentrations in phantoms in the cases of measurements using the microneedle and the ordinary Raman measurement. The AEFs of microneedle with and without Ag coating are calcu-

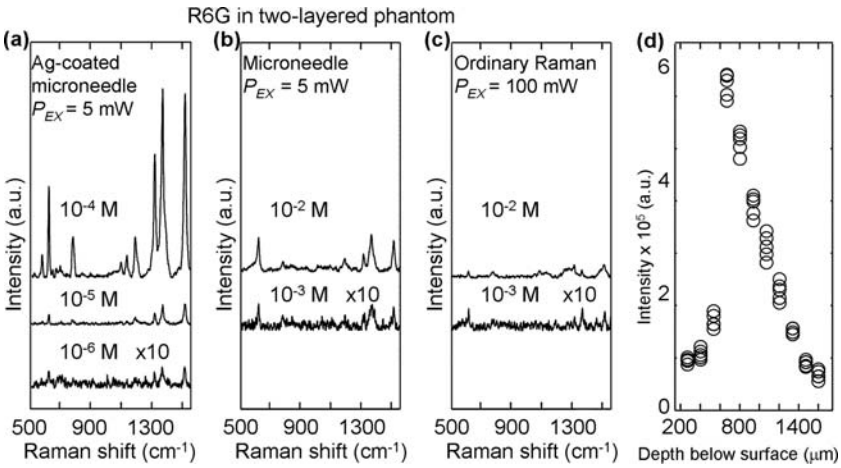

Figure 2 SERS spectra of R6G buried inside phantoms at 760 μm below the surface measured by using (**a**) Ag-coated microneedle (R6G concentrations: 10^{-4}, 10^{-5}, and 10^{-6} M; P_{EX}: 5 mW), (**b**) microneedle (R6G concentrations: 10^{-2}, and 10^{-3} M; P_{EX}: 5 mW), and (**c**) ordinary Raman (R6G concentrations: 10^{-2}, and 10^{-3} M; P_{EX}: 100 mW). P_{EX} means the excitation power. The legend "×10" indicates that the intensities of the corresponding spectrum have been multiplied by 10 to facilitate visualization. (**d**) Dependence of laser focusing depth below the two-layer phantom surface (10^{-5} M of R6G buried in bottom layer) on the SERS intensity of R6G at a Raman peak of 1365 cm^{-1}.

lated to be 2×10^4, and 40, respectively, with respect to the ordinary Raman measurement without the microneedle. Thus, the Ag-coated microneedle-based SERS probe enables high-sensitive detection of test molecules buried deeper than 700 μm in a tissue-like phantom despite the loss incurred in the presence of light scatterers and absorbers.

The AEF of the Ag film coated stainless steel microneedle is 500 times higher in magnitude than that of the stainless steel microneedle without any coating. This improvement can be attributed to the surface enhancement effect caused by the fact that dielectric constant of Ag has a much larger absolute value for the real part and smaller imaginary part ($\varepsilon_1 = -23.4$ and $\varepsilon_2 = 0.38$ [17]) than stainless steel ($\varepsilon_1 = -10.24$ and $\varepsilon_2 = 19.2$ [20]). Such enhancement accounts for the higher R6G SERS intensity measured by Ag-coated microneedle compared to that without Ag coating (Figure 2). Thus, electromagnetic enhancement is resulted for the incident excitation field and the emitted Raman signal for R6G molecules in close vicinity to the Ag surface. The AEF value of 2×10^4 achieved in case of the Ag coated microneedle is comparable to that reported [21] in a different experimental setup in which about an enhancement factor of 10^4 was achieved using a Ag-coated tip. Our Ag-coated microneedle-based SERS probe allows direct SERS measurements of analyte molecules in phantoms without the introduction of nanoparticles or the requirement of removing the needle for testing, although at an expense of a reduced AEF due to light absorption and scattering in the phantom layers. Moreover, the microneedle creates a small opening between the two arms of the microneedle that may allow a portion of excitation light and Raman light to pass through the top phantom layer with minimum attenuation from absorption and scattering. As a result, the Raman measurement acquired by using the microneedle without Ag film [Figure 2(b)] is higher, with an AEF value of 40, in comparison to the ordinary Raman measurement [Figure 2(c)].

The feasibility of using the Ag-coated microneedle-based SERS probe to detect glucose was also investigated (Figure 3). Figure 3(a) compares the SERS spectra of different glucose concentrations, including 0, 5, and 25 mM (buried inside the bottom phantom layers) measured by using the Ag-coated microneedle, and the ordinary Raman spectrum of crystalline glucose. These spectra were obtained by averaging data from five different microneedles and phantom locations with a standard deviation of less than 10%. Note that the Ag-coated microneedle was incubated with 1-decanethiol (1 mM) in ethanol for 16 hours prior to SERS measurements because decanethiol-modified Ag was reported in other type of SERS substrates [5] for effective SERS glucose detection. Prominent Raman peaks are observed at

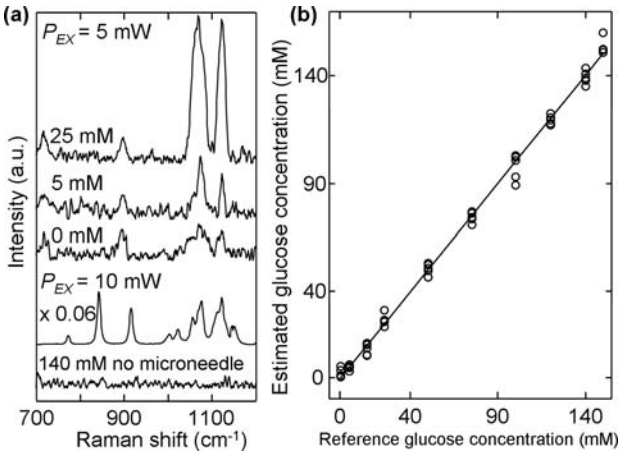

Figure 3 (**a**) SERS spectra for the glucose concentrations of 0, 5, and 25 mM positioned inside phantom at 760 μm below the surface measured by using the Ag-coated microneedle-based probe at an excitation power of 5 mW, and ordinary Raman of crystalline glucose and glucose phantom at concentration of 140 mM without microneedle at an excitation power of 10 mW. (**b**) Correlation between estimated glucose concentrations and reference glucose concentrations, in which the former values were estimated by PLS-LOO method from SERS spectra measured in phantom using the Ag-coated microneedle-based probe.

about 1076 and 1124 cm^{-1}, which can be attributed to the C–C, and C–O–H deformation of glucose [22], respectively. Raman intensities at these positions increase with the glucose concentration, in contrast to the unchanged Raman intensity peaks at 714, 889, 1073 and 1128 cm^{-1} attributed to 1-decanethiol adsorbed on the Ag-coated surface (concentration at 0 mM). Raman peaks at 914, and 840 cm^{-1} are only noted for glucose in crystalline state, which is also similar to other substrates [5] reported in the literature. In contrast, without this SERS probe, glucose Raman peaks cannot be detected at all as shown by the spectrum at the bottom of Figure 3(a).

Figure 3(b) correlates the estimated glucose concentrations, C_{est}, from the SERS intensities with reference to the known glucose concentrations, C_{ref}, (from 0 to 150 mM) by using the PLS-LOO cross validation technique. Raman intensities at 1076 and 1124 cm^{-1} were selected for the estimation of glucose concentrations by calculating the area under these Raman peaks after fluorescence background removal. An RMSE of 3.3 mM is realized in our Ag-coated microneedle-based SERS probe. These results show the potential for sensitive biomolecules detection.

The RMSE of 3.3 mM is comparable to that obtained in other similar substrates for SERS glucose detection. For example, RMSEs of 1.8 mM and 3.3 mM were achieved with and without decanethiol modification [5] for prediction in glucose solution using Ag-coated nanospheres. The slightly larger

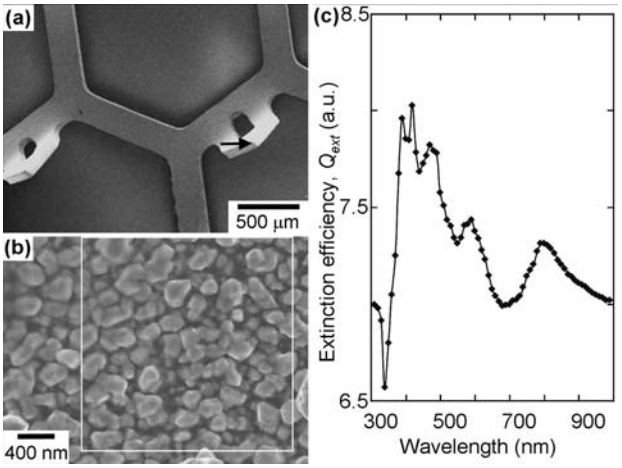

Figure 4 (**a**) FESEM image of the Ag-coated microneedle. (**b**) Representative surface morphologies of Ag coated on the microneedle tip [as indicated by the arrow in (a)] and other locations in the microneedle after removal from a phantom. (**c**) Extinction efficiency of Ag morphology [outlined by the white rectangle in (b)] on the microneedle calculated by using discrete dipole approximation (DDA).

RMSE in our strategy could be attributed to two possibilities. The first is that a portion of excitation and Raman light had to go through the 760 μm top layer thus subject to light absorption and scattering in this layer. The second is that Ag on the microneedle, synthesized by Tollen's method, has a larger surface roughness, as shown by the Ag morphologies in the FESEM image [Figure 4(a) and (b)] that could lead to higher Raman intensity variations as compared to Ag film fabricated by the vaporization method [23]. The Tollen's method is chosen in this study, since this technique is cost-effective [24] in scaling up for potential mass production in the future, and flexible in the coating of three-dimensional geometries [24] with film morphologies that adhere to the substrates even after insertion and withdrawal [Figure 4(b)]. In addition, this Ag morphology provides a local peak at about 800 nm in the extinction efficiency spectrum [Figure 4(c)], which contributes to the effective SERS enhancement as shown in our experimental results (Figures 2 and 3). This Ag-coated microneedle-based SERS probe demonstrates the capability to detect glucose concentrations between 5 and 150 mM, which is comparable to normal and severe glucose concentrations in blood [5]. The proposed method promises for the minimally invasive *in vivo* intradermal SERS measurements without the needs of injecting nanoparticles, drawing of body fluid, using chemicals and laboratory equipment such as anticoagulant, centrifuge. These results warrant for the optimization of this SERS strategy in the following areas to further improve the detection sensitivity and accuracy: (1) the thickness, surface roughness, and type of materials for SERS-active films coated on the microneedle, (2) different designs of the microneedle, and (3) *ex vivo* and *in vivo* measurements in animal model.

4. Conclusion

In conclusion, we realize Ag coated microneedle-based SERS probe for sensitive detection of test molecules buried at a depth of more than 700 μm in a two-layered phantom mimicking the light absorption and scattering properties of human skin. The quantification of glucose concentration using this method demonstrates the potential application of the Ag-coated microneedle-based probe for *in vivo* intradermal SERS measurements.

Acknowledgements This research was funded by the Singapore Lee Kuan Yew (LKY) start-up grant. The authors are also grateful to the LKY research fellowship (Clement Yuen) for sponsoring him to carry out his postdoctoral research and the New Investigator Grant (Project No. NMRC/NIG/1044/2011) funded by the National Medical Research Council (NMRC) in Singapore (Quan Liu).

Author biographies Please see Supporting Information online.

References

[1] T. S. Kupper and R. C. Fuhlbrigge, Nat. Rev. Immunol. **4**, 211–222 (2004).
[2] S. J. Moon and S. S. Lee, J. Micromech. Microeng. **15**, 903–933 (2005).
[3] C. Krafft, B. Dietzek, and J. Popp, Analyst **134**, 1046–1057 (2009).
[4] V. Kalchenko, Y. Kuznetsov, I. Meglinski, and A. Harmelin, J. Biomed. Opt. **17**, 050502 (2012).
[5] K. E. Shafer-Peltier, C. L. Haynes, M. R. Glucksberg, and R. P. V. Duyne, J. Am. Chem. Soc. **125**, 588–593 (2002).
[6] C. L. Zavaleta, B. R. Smith, I. Walton, W. Doering, G. Davis, B. Shojaei, M. J. Natan, and S. S. Gambhir, Proc. Natl. Acad. Sci. **106**, 13511–13516 (2009).
[7] P. V. Asharani, Y. L. Wu, and S. Valiyaveetil, Nanotechnology **19**, 255102 (2008).
[8] J. Dong, Q. Chen, C. Rong, D. Li, and Y. Rao, Anal. Chem. **83**, 6191–6195 (2011).
[9] J. J. Niu, M. G. Schrlau, G. Friedman, and Y. Gogotsi, Small **7**, 540–545 (2011).
[10] V. V. Yuzhakov, Drug Deliv. Technol. **10**, 32–36 (2010).
[11] N. J. Borys and J. M. Lupton, J. Phys. Chem. C **115**, 13645–13659 (2011).

[12] J. S. Dam, C. B. Pedersen, T. Dalgaard, P. E. Fabricius, P. Aruna, and S. Andersson-Engels, Appl. Opt. **40**, 1155–1164 (2001).
[13] C. Yuen and Q. Liu, J. Biomed. Opt. **17**, 017005 (2012).
[14] R. Wolthuis, G. C. H. Tjiang, G. J. Puppels, and T. C. B. Schul, J. Raman Spectrosc. **37**, 447–466 (2006).
[15] H. Abdi, Partial least square regression (PLS regression), in: Encyclopedia for research methods for the social sciences, M. L. Beck, A. Bryman, and T. Futing (eds.) (Thousand Oaks, California Sage Publication, 2003), pp. 792–795.
[16] M. A. Yurkin and A. G. Hoekstra, J. Quant. Spectrosc. Radiat. **112**, 2234–2247 (2011).
[17] P. B. Johnson and R. W. Christy, Phys. Rev. B **6**, 4370–4379 (1972).
[18] C. Yuen, W. Zheng, and Z. Huang, J. Raman Spectrosc. **41**, 374–380 (2009).
[19] B. W. Brian and M. S. Patterson, J. Biomed. Opt. **11**, 041102 (2006).
[20] B. Karlsson and C. G. Ribbing, J. Appl. Phys. **53**, 6340–6346 (1982).
[21] T. Schmid, B. S. Yeo, G. Leong, J. Stadler, and R. Zenobi, J. Raman Spectrosc. **40**, 1392–1399 (2009).
[22] P. D. Vasko, J. Blackwell, and J. L. Koenig, Carbohyd. Res. **23**, 407–416 (1972).
[23] Z. Wang, S. Pan, T. D. Krauss, H. Du, and L. J. Rothberg, Proc. Natl. Acad. Sci. **100**, 8638–8643 (2003).
[24] A. Antonello, B. Jia, Z. He, D. Buso, G. Perotto, L. Brigo, G. Brusatin, M. Guglielmi, M. Gu, and A. Martucci, Plasmonics **7**, 633–639 (2012).